# THz diffractive focusing structures for broadband application

K. Liebert,[*1] M. Rachon,[1] J. Bomba,[1] A. Sobczyk,[1] P. Zagrajek,[2] M. Sypek,[1] J. Suszek,[1] and A. Siemion[1]

[1]*Faculty of Physics, Warsaw University of Technology, 75 Koszykowa Str., 00-662 Warsaw, Poland*
[2]Institute of Optoelectronics, Military University of Technology, 2 Urbanowicz Str., 00-908 Warsaw, Poland

**Abstract**—Analysis of optical structures that can work for a broadband range of THz radiation is the aim of this article. Such structures can be designed as kinoforms of higher order or elements with an extended depth of focus, like axicons or light sword elements. A theoretical and experimental comparison of different optical elements for three significantly different frequencies is performed.

THz radiation possesses interesting features that make it desirable for security applications [1]. THz scanners [2] are already used at the airports and can detect concealed, dangerous items. This radiation is not ionizing, therefore, it is safe for living organisms [3-4] as opposed to commonly used X-rays. Lately, the THz postal scanner [5] has been demonstrated and enabled examination of the content of an envelope without opening it. Moreover, it is possible to determine whether the envelope does not contain any dangerous objects made of metal, wood, plastic or disturbing powders, but requires scanning with more than one frequency. For this reason, a lens is desirable, capable to shape the beam for few specific wavelengths that are drastically different (for example for $\frac{\lambda}{2}, \lambda, 2\lambda$).

The main drawback is that those THz detectors existing on the market have a low signal to noise ratio [6] and thus it is necessary to accurately focus incident radiation. In this case, beam shaping seems to be necessary and can be carried out by mirrors [7], refractive structures [8] or structures based on the phenomenon of diffraction [9]. Diffractive optical elements (DOEs) are characterized by lightness, small thickness and relatively low price.
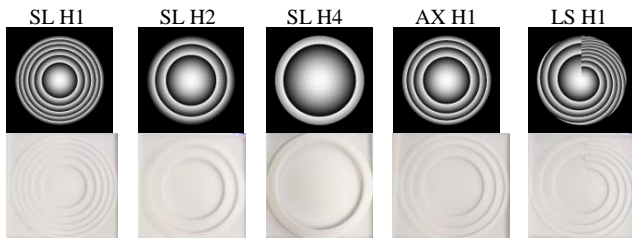


Fig. 1 Phase distribution of designed optical elements (upper row) corresponding to the depth map, where black introduces 0 and white $2p\pi$ phase shift, where $p = 1$, 2 or 4 and is the order of the kinoform. The photograph of 3D printed optical elements (lower row).

* E-mail: karolina.liebert@gmail.com

In this article DOEs working at different frequencies will be discussed – first, the comparison of spherical lens (SL) coded as kinoform [10] and high order kinoforms (HOKs) [11-12] and then elements with extended depth of focus – axicons (AX) [13] and light sword elements (LS) [14] (as 1st order kinoform structures).

Kinoform structures, due to their maximal phase shift of only $2\pi$, are for narrowband use only, because with illumination of different wavelengths than the design wavelength (DWL) they are characterized by chromatic aberration. A different approach to coding phase distribution is using high order kinoforms that combine the advantages of refractive and diffractive structures. This type of kinoform has the phase shift several times greater than $2\pi$. For this reason, it has achromatic properties like a refractive structure while retaining the advantages of a diffractive structure. Despite the fact that HOKs are several times thicker than first order kinoforms, they are still significantly thinner and lighter than refractive ones. However, the simulation algorithm should assume this thickness (corresponding to multiple wavelengths) and thus the mBPM (modified Beam Propagation Method) [15] is applied.

Table. 1. Formulas describing the phase distribution of designed optical elements. Here, $f$ is the designed focal length equal to 50 mm, $\lambda$ is the wavelength (DWL = 1 mm), $a = 0.028$, $d_2 = 90$, $f_1 = 40$, $f_2 = 80$.

| Element | Phase distribution ɸ |
|---------|----------------------|
| SL H1 | $-\frac{2\pi}{\lambda}\sqrt{r^2 + f^2}$ |
| SL H2 | $-\frac{\pi}{\lambda}\sqrt{r^2 + f^2}$ |
| SL H4 | $-\frac{\pi}{2\lambda}\sqrt{r^2 + f^2}$ |
| AX H1 | $-\frac{\pi}{\lambda a}ln|2a\sqrt{a^2r^4 + (1 - 2ad_2)r^2 + d_2^2 + 2a^2r^2} - 2ad_2 + 1$ |
| LS H1 | $-\frac{2\pi}{\lambda}\sqrt{r^2 + \left(f_1 + \frac{f_2\Theta}{2\pi}\right)^2} - \frac{2\pi}{\lambda}(f_1 + \frac{f_2\Theta}{2\pi})$ |

Another method of reducing chromatic aberrations is using structures that increase the depth of focus (like LS and AX structures). It can result in focusing all considered wavelengths in the same way into some line

segment along the optical axis. Thus, chromatic aberration will be reduced.

All optical elements were calculated in a non-paraxial approach. Phase distributions ϕ presented in the greyscale as depth maps (described with formulas given in Tab. 1) and photos of the designed structures are shown in Fig. 1.

Computer modeling for all structures was carried out (using Light Sword 6.0 software available in the Laboratory of Optical Information Processing) on arrays 4096 × 4096 pixels with the sampling 117 μm × 117 μm (which was determined by the resolution of a 3D printing machine). The structures were designed for the wavelength DWL=1mm. However, simulations were carried out also for: 0.5mm (600GHz) and 2mm (150GHz). The absorption coefficient strongly depended on the frequency (using polyamide 12 material was assumed) and was equal to: 0.5cm$^{-1}$ (@150GHz), 1 cm$^{-1}$ (@300GHz) and 7 cm$^{-1}$ (@600GHz), while the refractive index was equal to 1.59 for these frequencies.

The results of computer modeling compared to experimental evaluation are presented in Tables 2 and 3.
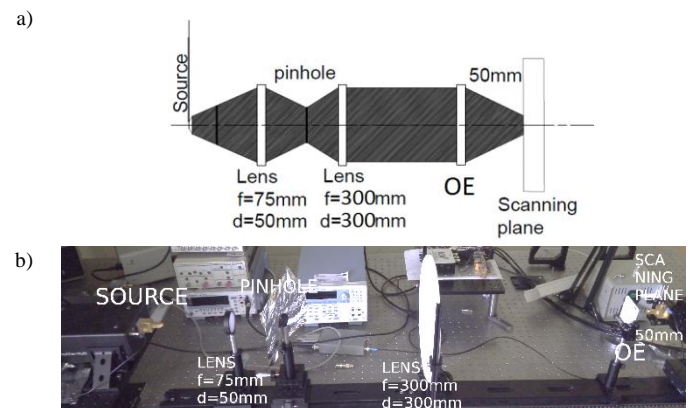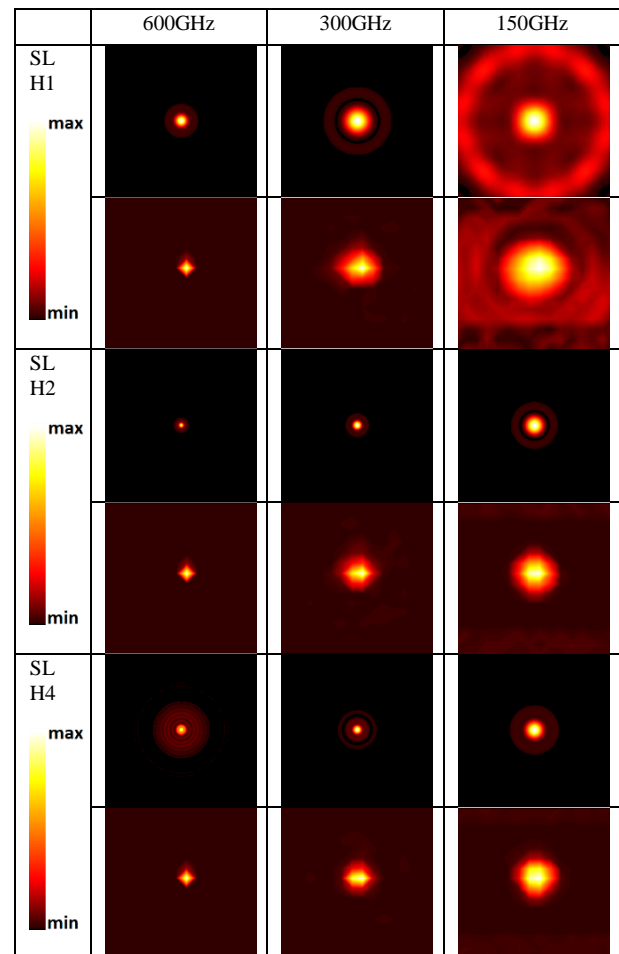
a)



b)



Fig. 2. The optical system in the experiment: a) a scheme and b) a photo.

The experimental optical system is presented in Fig. 2. THz radiation was provided by a VDI (Virginia Diodes, Inc., Charlottesville, VA, USA) frequency multiplier and illuminated a lens ($f$ =75mm, $d$=50 mm) that focused the incident light on a circular aperture with a diameter of 2mm. Then, at a distance of 300mm after pinhole a HDPE lens ($f$ =d of 300 mm) was placed forming a quasi-plane wave that illuminated the designed optical element (OE). Finally, the image was scanned at a distance of 50mm behind the structure (OE).

Measurements were performed for three frequencies: 150GHz, 300GHz and 600GHz. The power of generated radiation was equal to: 1mW, 0.8mW, and 40μW, respectively. The emitters were equipped with horn antennas which formed divergent beams.

The focal point was scanned with a Schottky diode detector also equipped with a horn antenna whose

aperture diameter was equal to: 8.4mm, 5.6mm and 2.4mm for frequencies 150GHz, 300GHz and 600GHz, respectively. The scanning step of the detector was 2mm. To measure the signal from the detector, a lock-in system (Stanford Research Systems SR830) was used, based on modulation at 187Hz.

Table 2. Intensity distributions being the results of computer modeling and experimental results of a spherical lens coded as a kinoform of first, second and fourth order . The size of the area is equal to 30mm.



All optical elements were manufactured using selective laser sintering (SLS) as a 3D printing method [16], using a polyamide 12 (PA12) material. The refractive index of PA12 for all frequencies is approximately equal to 1.59, which results in the thickness of the structure $1.69p$ mm, where $p$ = 1, 2 or 4 and is the order of the kinoform.

The experimental results showing intensity distribution are presented in Tab. 2 and Tab. 3. Due to the fact that different power of sources and different detectors for different wavelengths were used, the maximal value in the focal spot in the experimental part should not be compared between frequencies. Taking into account the fact that the scanning step was 2mm, we verified for each frequency if the relation between measured intensity

values for different elements were corresponding to the values calculated in numerical simulations. Any deviation of measured values from the simulation results corresponded to the sampling difference and relatively large scanning step. Radiation incoming to the detector could not be registered efficiently due to a different place and angle of the incident at this position beam.

It should be noticed that a smaller diameter of the focal spot for higher frequency corresponds to the theory describing the Airy disc size (proportional to the wavelenght). Moreover, SL designed as a kinoform of 1st order should not work for the frequency 150 GHz, which can be observed in Tab. 2.

Table 3. Intensity distributions being the results of computer modeling and experimental evaluation for axicon (AX) and light sword optical element (LS). The size of the area is equal to 30mm.
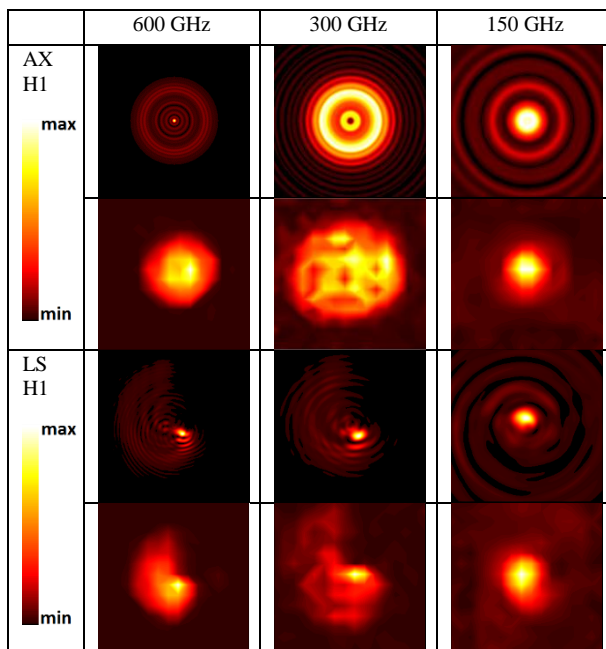


In conclusions, the main issue was to investigate if the designed optical elements: spherical lenses (as kinoforms of 2nd and 4th order), light sword optical element (LS) and axicon (AX) have better optical properties (focal spot and maximum intensity) then the Fresnel lens (spherical lens as a kinoform of 1st order). Each of the tested structures is characterized by better performance at 150GHz than SL H1 (except SL H4, which is related to a very high attenuation coefficient of PA12 material at 600GHz (both in computer modeling and in the experiment).

The axicon structure itself and experimental setup should be redesigned. Here, probably only the main zone was illuminated and therefore the nature of the structure is not maintained.

## References

[1] M.C. Kemp, P.F. Taday, B.E. Cole, J.A. Cluff, A.J. Fitzgerald, W.R. Tribe, International Society for Optics and Photonics **5070**, 44 (2003). https://doi.org/10.1117/12.500491
[2] D. Yavorskiy, J. Marczewski, K. Kucharski *et al*., Phot. Lett. Poland **4**(3), 100 (2012). http://photonics.pl/PLP/index.php/letters/article/view/4-36
[3] A.A. Angeluts, A.B. Gapeyev, M.N. Esaulkov *et al*., Quant. Electr. **44**(3), 247 (2014). http://iopscience.iop.org/article/10.1070/QE2014v044n03ABEH015337
[4] Q. Sun, Y. He, K. Liu, S. Fan, E.P. Parrott, E. Pickwell-MacPherson, Quant. Imag. Med. Surg. **7**(3), 345 (2017). http://qims.amegroups.com/article/view/15326/15541
[5] J. Suszek, A. Siemion, M. Bieda *et al*., IEEE Thz Sci. T. **5**, 15326 (2015). http://qims.amegroups.com/article/view/15326/15541
[6] M. Naftaly, R. Dudley, Opt. Lett. 34(8), 1213 (2009). https://www.osapublishing.org/ol/abstract.cfm?uri=ol-34-8-1213
[7] C. Bruckner, G. Notnia, A. Tünnermann, Optik **121**, 1 (2010). https://www.sciencedirect.com/science/article/pii/S0030402608001393?via%3Dihub
[8] J. Richter, A. Hofmann, L.-P. Schmidt, Proc. 31st Europ. Microw. Conf., London 2001. http://ieeexplore.ieee.org/document/4140002/
[9] E.D. Walsby, S. M. Durbin, D.R S. Cumming, R.J. Blaikie, Curr. App. Phys. **4**, 102 (2004). https://www.sciencedirect.com/science/article/pii/S1567173903001524
[10] J.A. Jordan Jr. *et al*, Appl Opt. **9**(8), 1883 (1970). https://doi.org/10.1364/AO.9.001883
[11] J.C. Marron, D.K. Angell, A.M. Tai, Intern. Soc. Opt. Photon. **1211**, 62 (1990). https://doi.org/10.1117/12.17930
[12] J. Suszek, A.M. Siemion, N. Błocki, M. Makowski, A. Czerwiński, J. Bomba, P. Zagrajek *et al*., Opt. Expr. **22**(3), 3137 (2014). https://doi.org/10.1364/OE.22.003137
[13] J. Sochacki, A. Kołodziejczyk, Z. Jaroszewicz, S. Bara, App. Opt. **31**(25), 5326 (1992). https://doi.org/10.1364/AO.31.005326
[14] A. Kołodziejczyk, S. Bará, Z. Jaroszewicz, M. Sypek, J. Modern Opt. **37**(8), 1283 (1990). https://doi.org/10.1080/09500349014551431
[15] M. Sypek, Opt. Commun. **116**, 43 (1995). https://doi.org/10.1016/0030-4018(95)00027-6
[16] J.P. Kruth, X. Wang, T. Laoui, L. Froyen, Assembly Autom. **23**(4), 357 (2003). https://doi.org/10.1108/01445150310698652